Non-destructive coherence measurements with double pinholes at FLASH2

THOMAS WODZINSKI[1,2,*], **MABEL RUIZ-LOPEZ**[2], **MASOUD MEHRJOO**[2], **BARBARA KEITEL**[2], **MARION KUHLMANN**[2], **MACIEJ BRACHMANSKI**[2], **SWEN KÜNZEL**[1], **MARTA FAJARDO**[1], **AND ELKE PLÖNJES-PALM**[2]

[1]*GoLP/Instituto de Plasmas e Fusão Nuclear, Instituto Superior Técnico, 1049-001 Lisboa, Portugal*
[2]*Deutsches Elektronen-Synchrotron DESY, Notkestrasse 85, 22607 Hamburg, Germany*
[*]*thomas.wodzinski@tecnico.ulisboa.pt*

Abstract:

Since 2016 FLASH at DESY in Hamburg operates the variable-gap undulator beamline FLASH2 as a user facility. Young's double pinhole measurements were performed at photon beamline FL24 downstream of the Kirkpatrick-Baez focusing optics, which were installed in 2017. FLASH2 was characterized at wavelengths of 8, 13.5 and 18 nm and under different machine settings. The coherence length was determined from the interference pattern of several pinhole pair separationscovering the width of the beam. A blind deconvolution algorithm was implemented to determine the coherence function from the partially coherent interference pattern. Simulations of the patterns including the Kirkpatrick-Baez focusing optics were implemented with WavePropaGator (WPG), a software for X-ray wavefront propagation simulations developed at the European XFEL. We present first results of these coherence measurements and simulations.

1. Introduction

2. Basic equations of optical coherence

In a coordinate system $\vec{r} = (x, y, z)$ a beam with a scalar electric field $E(\vec{r}, t)$ propagates longitudinally along the z-axis. The transverse coordinates are (x, y) and t is the arrival time of the signal at a particular location z.

The mutual coherence function (MCF) [1] between two points r_1 and r_2 is

$$\Gamma(\vec{r}_1, \vec{r}_2, t_1, t_2) = \langle E(\vec{r}_1, t_1), E^*(\vec{r}_2, t_2) \rangle_T \tag{1}$$

with $\langle \rangle_T$ denoting the ensemble average over many radiation pulses over a time interval T and * the complex-conjugate.

The radiation intensity is $I(\vec{r}, t) = \Gamma(\vec{r}, \vec{r}, t, t)$.

The complex degree of (mutual) coherence (CDC) γ is defined as the normalized mutual coherence function [2, eq.4]:

$$\gamma(\vec{r}_1, \vec{r}_2, t_1, t_2) = \frac{\Gamma(\vec{r}_1, \vec{r}_2, t_1, t_2)}{\sqrt{I(\vec{r}_1, t_1)}\sqrt{I(\vec{r}_2, t_2)}} \tag{2}$$

where $\gamma(\vec{r}_1, \vec{r}_2, 0)$ describes transverse or spatial coherence, while $\gamma(0, 0, \tau)$ describes longitudinal or temporal coherence.

The spatial or transverse coherence length ξ is defined as the root mean square (rms) width of the modulus of the CDC [2, eq.5] along the distance d between two points:

$$|\gamma_{12}^{\text{eff}}(d)| \propto \exp\left[-\frac{d^2}{2\xi_x^2}\right] \tag{3}$$

It can be helpful to rather use the term coherence area [3, fig. 11.2] to avoid confusion with the coherence length L_c calculated from the temporal coherence time.

The size of the beam can be described by its rms width σ_x:

$$I(x) \propto \exp\left[-\frac{x^2}{2\sigma_x^2}\right] \tag{4}$$

A measure of the degree of coherence is the ratio q_x between the coherence length ξ_x and the rms width of the beam σ_x [4]:

$$q_x = \frac{\xi_x}{\sigma_x} \tag{5}$$

3. Young's double pinhole experiment of a beam with a flat wave front

The intensity profile $I(\vec{u})$ of Youngs' double pinhole experiment [5, fig. 5.12] can be described by the interference equation [6, eq. (2.5-4)]:

$$I(\vec{u}) = I_1(\vec{u}) + I_2(\vec{u}) + 2\sqrt{I_1(\vec{u})}\sqrt{I_2(\vec{u})} \cdot |\gamma_{12}(\tau)| \cdot \cos\left(\delta(\vec{u}) + \alpha_{12}(\tau)\right) \tag{6}$$

with the time delay τ between the signals from both pinholes on the detector, the intensities $I_{1,2}$ of propagated fields $E_{1,2}$ from pinhole 1 and 2, the rapidly changing phase $\delta(\vec{u})$ of γ_{12} describing the interference fringe pattern and the slowly changing phase $\alpha_{12}(\tau)$.

Under paraxial conditions, with tiny pinholes [5, eq. (5.2-34)] and with a small path length difference due to the time delay being smaller than the coherence time $\tau < \tau_c$ we find for $\delta(\vec{u})$ and $\alpha_{12}(\tau)$:

$$\delta(\vec{u}) \approx 2\pi \frac{\vec{u} \cdot \vec{d}}{\lambda z} \tag{7}$$

and

$$\alpha_{12}(\tau) \approx \alpha_{12}(0) \tag{8}$$

Let the intensity $I_i(\vec{u})$ of pinhole i with diameter D_i on the screen $\vec{u}$ be described by a constant factor I_i and a normalized profile $\hat{I}_{D_i}(\vec{u})$:

$$I_i(\vec{u}) = I_i \cdot \hat{I}_{D_i}(\vec{u}) \tag{9}$$

In the far-field from the pinholes the intensity profiles of both pinholes can be approximated to overlap at the detector:

$$\hat{I}_{D_1}(\vec{u}) = \hat{I}_{D_2}(\vec{u}) \tag{10}$$

The intensity profile of a pinhole in the far-field can be described by the Airy function $A_{D_i}(\vec{u})$:

$$\hat{I}_{Di}(\vec{u}) = \left|A_{D_i}(\vec{u})\right|^2 \tag{11}$$

With both pinholes having the same diameter $D = D_1 = D_2$ equation 6 can be written as:

$$I(\vec{u}) = (I_1 + I_2) \cdot I_D(\vec{u}) \left[1 + \left|\gamma_{12}^{\text{eff}}(\tau)\right| \cdot \cos\left(2\pi \frac{\vec{u} \cdot \vec{d}}{\lambda z} + \alpha_{12}(0)\right)\right] \tag{12}$$

with the effective CDC $\gamma_{12}^{\text{eff}}(\tau)$ defined as:

$$\gamma_{12}^{\text{eff}}(\tau) = 2\frac{\sqrt{I_1 \cdot I_2}}{I_1 + I_2} \cdot \gamma_{12}(\tau) \tag{13}$$

Visibility $\mathcal{V}$ is defined as:

$$\mathcal{V} = \frac{I_{\max} - I_{\min}}{I_{\max} + I_{\min}} \tag{14}$$

At the center of the screen, where $\tau = 0$, we can approximate:

$$\gamma_{12}^{\text{eff}}(\tau) \approx \gamma_{12}^{\text{eff}}(0) \tag{15}$$

We therefore can determine the modulus of the CDC $|\gamma_{12}(0)|$ from the central visibility:

$$\mathcal{V} = 2\frac{\sqrt{I_1}\sqrt{I_2}}{I_1 + I_2} |\gamma_{12}(0)| = \left|\gamma_{12}^{\text{eff}}(0)\right| \tag{16}$$

Usually, one would fit $|\gamma_{12}^{\text{eff}}(0)|$ as a function of the the pinhole separation d with a Gaussian to determine the transverse coherence length ξ_x from the rms width of this fit (see equation 3) [7, fig.4].

These approximations require the wave front to be flat.

4. Young's double pinhole experiment of a beam with a curved wave front

If the pinhole pair is not in the focus of the beam the visibility cannot be used as a measure of the CDC. The intensities of each pinhole cannot be assumed to overlap anymore:

$$\hat{I}_{D_1}(\vec{u}) \neq \hat{I}_{D_2}(\vec{u}) \tag{17}$$

The focus is located upstream before the pinhole pair at $z_0 = 0$ in such a way that they are being illuminated by a diverging beam with a curved wave front.

Huygens-Fresnel principle [8]:

$$E(\vec{u}, z_2) = \iint P_z(\vec{u}, \vec{s})E(\vec{s}, z_1)\,d\vec{s} \tag{18}$$

with the propagator P_z:

$$P_z(\vec{u}, \vec{s}) = \frac{k}{2\pi i}\frac{e^{ikr}}{r} \tag{19}$$

Fresnel-propagator over distance z:

$$P_z(\vec{u}, \vec{s}) = \frac{k}{2\pi i}\frac{e^{ikz}}{z} \exp\left[ik\frac{|\vec{u}|^2 + |\vec{s}|^2 - 2\vec{u}\cdot\vec{s}}{2z}\right] \tag{20}$$

Fraunhofer-propagator over distance z:

$$P_z(\vec{u}, \vec{s}) = \frac{k}{2\pi i}\frac{e^{ikz}}{z} \exp\left[ik\frac{|\vec{u}|^2 - 2\vec{u}\cdot\vec{s}}{2z}\right] \tag{21}$$

Let the wavefront at the pinhole plate be quadratic:

$$E(\vec{s}, z_1) = E_0 \exp\left[ik\frac{|\vec{s}|^2}{2z_1}\right] \tag{22}$$
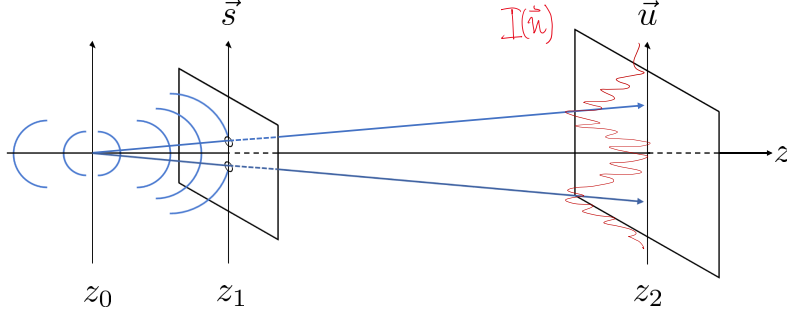
Fig. 1. A diverging beam with a focus at z_0 with a curved wave front illuminates a pinhole pair at z_1. The resulting interference pattern $I(\vec{u})$ on the screen at z_2 samples the curvature.

Propagating the field $E(\vec{s}, z_1)$ at z_1 to z_2 over the distance $z = \Delta z_{12} = z_2 - z_1$ using Fresnel approximation (eq. 20):

$$E(\vec{u}, z_2) = \iint P_z(\vec{u}, \vec{s}) E(\vec{s}, z_1)\, d\vec{s} \tag{23}$$

$$= \iint \frac{k}{2\pi i} \frac{e^{ikz}}{z} \exp\left[ik \frac{|\vec{u}|^2 + |\vec{s}|^2 - 2\,\vec{u}\cdot\vec{s}}{2z}\right] E(\vec{s}, z_1)\, d\vec{s} \tag{24}$$

Inserting 22 into 24 leads to the Fresnel scaling theorem for propagating a spherical wave front ([9, "Appendix B", pp.397-400]):

$$E(\vec{u}, z_2) = \iint \frac{k}{2\pi i} \frac{e^{ikz}}{z} \exp\left[ik \frac{|\vec{s}|^2}{2z_M}\right] \exp\left[ik \frac{|\vec{u}|^2 - 2\,\vec{u}\cdot\vec{s}}{2z}\right] E_0\, d\vec{s} \tag{25}$$

with the scaled distance z_M:

$$z_M = \frac{z_1 \cdot z}{z_1 + z} \tag{26}$$

Propagating through one of the two circular pinholes located at $s = +d/2$ away from the optical axis in the plane at z_1 with Diameter D:

$$E(\vec{u}, z_2) = \iint_{d/2-D/2}^{d/2+D/2} \frac{k}{2\pi i} \frac{e^{ikz}}{z} \underbrace{\exp\left[ik \frac{|\vec{s}|^2}{2z_M}\right]}_{\longrightarrow 1,\ \text{for Fraunhofer}} \exp\left[ik \frac{|\vec{u}|^2 - 2\,\vec{u}\cdot\vec{s}}{2z}\right] E_0\, d\vec{s} \tag{27}$$

If the quadratic term $|\vec{s}|^2$ in equation 25 can be neglected we transition from Fresnel to Fraunhofer diffraction (see [6], p.46), which requires:

$$k\frac{(d/2 \pm D/2)^2}{2z_M} \ll \pi \tag{28}$$

With $k = 2\pi/\lambda$, the pinhole separation d therefore has to fulfill the following condition:

$$|d| \ll 2\sqrt{\lambda z_M} - D \tag{29}$$

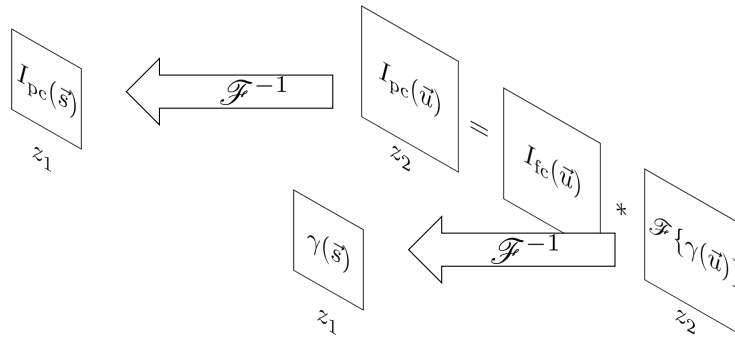## 5. Deconvolution-method to recover the fully coherent intensity

Fig. 2. Deconvolution method to determine the coherence length ξ as the rms width of the modulus of the complex degree of coherence $|\gamma(\vec{r})|$ at the pinhole plate position.

The measured partially coherent intensity at the detector $I_{\mathrm{pc}}(\vec{u})$ can be expressed as a convolution of the fully coherent intensity $I_{\mathrm{fc}}(\vec{u})$ with the Fourier-transformed of the CDC $\mathscr{F}\{\gamma(\vec{u})\}$ [10, eq.33]:

$$I_{\mathrm{pc}}(\vec{u}) = I_{\mathrm{fc}}(\vec{u}) * \mathscr{F}\{\gamma(\vec{u})\} \tag{30}$$

To determine the modulus of the CDC $\gamma(\vec{s})$ at the pinhole plate position z_1 we apply the inverse Fourier-transform to back-propagate.

The transverse coherence length ξ is the rms width of $|\gamma(\vec{s})|$ (see equation 3).

6. Experiment

Double pinholes with a diameter of $10\,\mu\mathrm{m}$ were illuminated at the beamline FL24 of FLASH2 positioned 1067 mm downstream of a focus produced by the Kirkpatrick-Baez focusing optics "KAOS" which is equipped with bendable mirrors. The experiment had different configurations. First, by using a Hartmann-WFS the focus was set to be at the position where a PMMA setup would be placed to create imprints along the caustic.

After the focus was established the end of the beamline was changed to replace the WFS with a XUV detector, a Princeton Instruments PIXIS XO-1024B with 1024x1024 pixels of

13 μm × 13 μm size, positioned 5781 mm from the position of the pinhole-plate which was itself 1067.5 mm downstream of the PMMA focus.

The work on the PMMA imprints was done in collaboration with a group from the Institute of Physics, Academy of Sciences of the Czech Republic from Prague around Jaromír Chalupský. They did similar measurements at LCLS [11].

After the PMMA imprints were performed the setup was moved out of the beampath and the pinhole plate was inserted. A fluorescent coating on a plate attached to the pinhole plate allowed an additional characterization of the beam size and position with an optical camera. The pinhole plate was movable in the transverse plane, allowing the positioning of several pinhole pairs ranging from 107 μm to 1557 μm in horizontal and vertical configuration to the beam.

For each pinhole pair consecutive single-shot measurements were recorded over a time of around 5 minutes. The optical beamline cameras recording the fluorescent screen were attached to the data acquisition system (DAQ). Each recorded image had a timestamp. These were later correlated in the data processing with the recorded images of the XUV camera. Background images were recorded with the beam hitting the fluorescent screen between two pinhole pairs.

WFS measurements were done before and after each PMMA measurement, which lasted several hours each.

A second measurement for each pinhole pair was done with the focus changed in such a way, that the beam size at the pinhole position had around half the size than before.

FLASH2 was set to operate at three different wavelengths, 8 nm, 13.5 nm and 18 nm. The machine settings are listed in table 1.
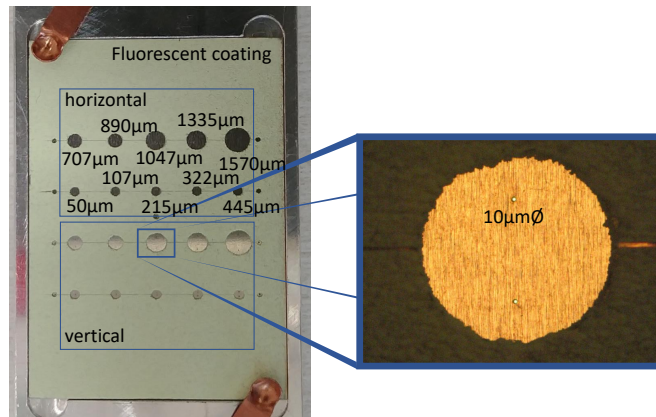

Fig. 3. Double pinhole plate with fluorescent coating. An microscope image shows the pinholes with a diameter of 10 μm

7. Data processing

Since the beamline cameras were recording the images into the data acquisition system, each recorded shot of the fluorescent screen had a timestamp associated to them. The images of the XUV detector were also captured by the DAQ, but were out of sync. The corresponding timestamp for each XUV image had to be determined by hand. With the correct timestamp
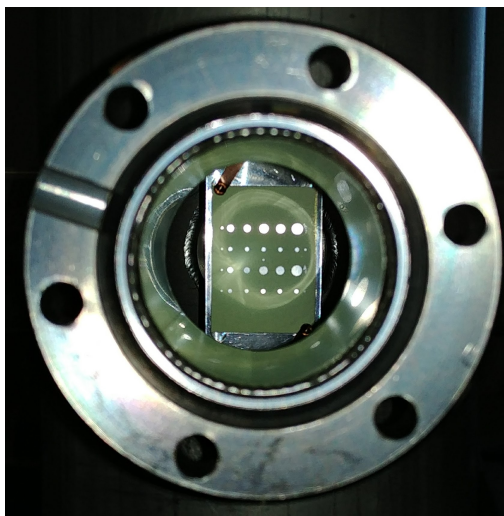
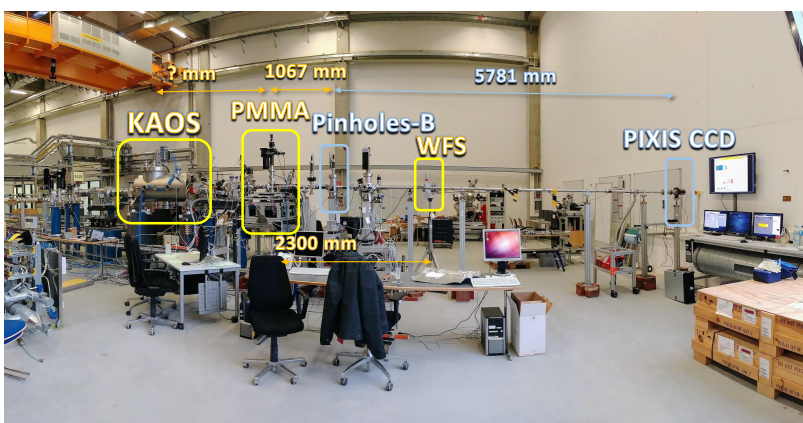Fig. 4. Double pinhole plate with fluorescent coating mounted inside a movable chamber.

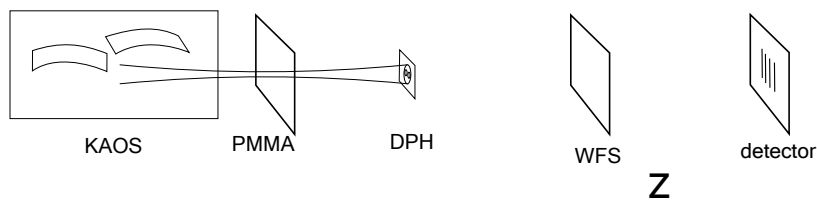Fig. 5. Double pinhole setup at beamline FL24 at FLASH2/DESY

Fig. 6. Double pinhole setup at beamline FL24 at FLASH2/DESY

run	26.11.2017	27.11.2017	29.11.2017
Wavelength	18 nm	8 nm	13.5 nm
# bunches	1	1	1
bunch charge	0.15 nC, 1003 kHz	0.15 nC, 1003 kHz	0.20 nC, 1003 kHz
	1010.59 MeV	1012.34 MeV	1046.93 MeV
Energy in the tunnel	77.4 µJ	53.7 µJ	527 µJ
Energy in the hall	66.7 µJ	45.1 µJ	111 µJ
Undulators	7 Undulators (8 to 14)	12 Undulators (3 to 14)	12 undulators (3 to 14)
Tapering	?	no tapering	quadratic tapering last 6 undulators
Attenuator	empty	empty	1.62×10^{-3} mbar Xe in attenuator
Filters	Nb 405 nm or Nb 197 nm	empty	empty

Table 1. Machine settings of FLASH2 during the measurements

known, each shot could be correlated with beam energies and positions provided by diagnostics in the beamline. As can be seen in figure 7 the
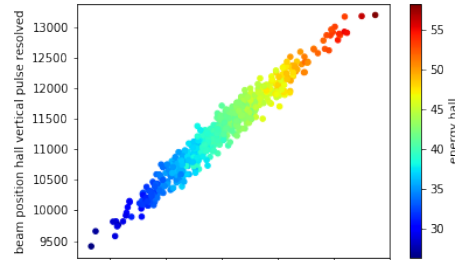
Fig. 7. Example of the linear beam position dependence on the beam energy from shot to shot.

The rotation of each image had to be slightly corrected by around ±1° to align the fringes of the interference pattern vertically. The images of the vertically aligned pinhole pairs were rotated by 90°.

8. Beam size at the pinhole plate

By solving the Fresnel-Kirchoff integral [12] the beam was back-propagated to the pinhole-plate position for each of the three machine settings. The WFS was in a distance of 1232 mm from the DPHs. Figure 8 shows the profile for each recorded wavelength in the left column. The center and right column show example images of the beam illuminating the pinhole and the surrounding fluorescent screen. In the center column the image corresponds to the same focus setting as in

the left column, except for the 8 nm case, where the beam was set smaller. The KB optic was changed such, that the beam diameter would be approximately half as large. This small beam can be seen in the right column. All images show the beam width in D4σ (width × height). The back-propagation shows the beam in upstream direction, while the images taken with the optical camera are facing downstream. That explains why the profiles are flipped along the vertical axis to each other.

9. Analysis

From the experimental geometry we calculate a scaled distance of $z_M \approx 0.85$ (with $z_p = 6\,\text{m}$ and $z_0 = 1\,\text{m}$), $\lambda = 13.5\,\text{nm}$ and $w = 10\,\mu\text{m}$). Using equation (29) this results in a cut-off value to apply Fraunhofer diffraction for the pinhole separation of $D_{cut-off} \approx 20\,\mu\text{m}$. All available pinhole separations are larger than this value, which means, that the central visibility cannot be used to determine the CDC γ and from its rms width the coherence length ξ.

Therefore, the deconvolution method has to be applied.

10. Results and Discussion

10.1. Single-shot analysis

10.2. beam and wave front stability

10.3. coherence

11. Future work

References

1. Z. Huang, "Brightness and Coherence of Synchrotron Radiation and FELs," in *Proceedings, 4th International Particle Accelerator Conference (IPAC 2013): Shanghai, China, May 12-17, 2013,* (2013), p. MOYCB101.
2. K. Bagschik, R. Frömter, L. Müller, W. Roseker, J. Bach, P. Staeck, C. Thönnißen, S. Schleitzer, M. H. Berntsen, C. Weier, R. Adam, J. Viefhaus, C. M. Schneider, G. Grübel, and H. P. Oepen, "Spatial coherence determination from the fourier analysis of a resonant soft x-ray magnetic speckle pattern," Opt. Express **24**, 23162–23176 (2016).
3. O. Svelto, *Principles of Lasers* (Springer US, 2010).
4. L. Mandel and E. Wolf, *Optical coherence and quantum optics* (Cambridge university press, 1995).
5. Goodman, *Statistical Optics 2e* (John Wiley & Sons, 2015).
6. M. C. T. Bahaa E.A. Saleh, *Fundamentals of Photonics* (Wiley John + Sons, 2007).
7. A. Singer, F. Sorgenfrei, A. P. Mancuso, N. Gerasimova, O. M. Yefanov, J. Gulden, T. Gorniak, T. Senkbeil, A. Sakdinawat, Y. Liu, D. Attwood, S. Dziarzhytski, D. D. Mai, R. Treusch, E. Weckert, T. Salditt, A. Rosenhahn, W. Wurth, and I. A. Vartanyants, "Spatial and temporal coherence properties of single free-electron laser pulses," Opt. Express **20**, 17480–17495 (2012).
8. M. Born, E. Wolf, and A. B. Bhatia, *Principles of Optics* (Cambridge University Pr., 2002).
9. D. Paganin, *Coherent X-Ray Optics*, Oxford Series on Synchrotron Radiation (OUP Oxford, 2006).
10. I. A. Vartanyants and I. K. Robinson, "Partial coherence effects on the imaging of small crystals using coherent x-ray diffraction," J. Physics: Condens. Matter **13**, 10593 (2001).
11. J. Chalupský, P. Boháček, T. Burian, V. Hájková, S. P. Hau-Riege, P. A. Heimann, L. Juha, M. Messerschmidt, S. P. Moeller, B. Nagler, M. Rowen, W. F. Schlotter, M. L. Swiggers, J. J. Turner, and J. Krzywinski, "Imprinting a focused x-ray laser beam to measure its full spatial characteristics," Phys. Rev. Appl. **4**, 014004 (2015).
12. B. FlÃűter, P. JuraniÄĞ, S. Kapitzki, B. Keitel, K. Mann, E. PlÃűnjes, B. SchÃďfer, and K. Tiedtke, "Euv hartmann sensor for wavefront measurements at the free-electron laser in hamburg," New J. Phys. **12**, 083015 (2010).

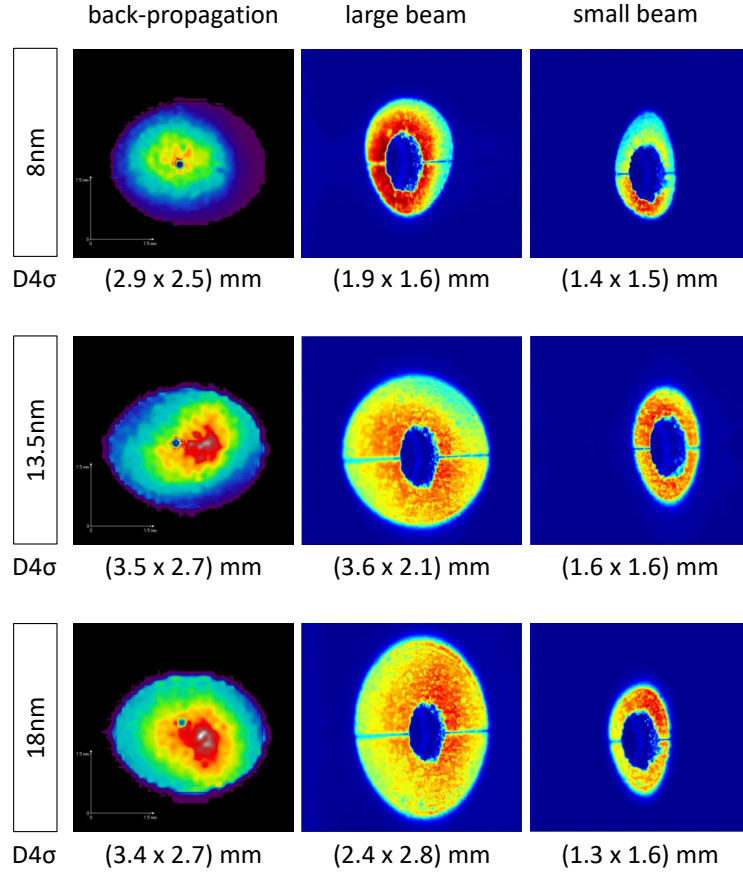|	back-propagation	large beam	small beam
8nm	(2.9 x 2.5) mm	(1.9 x 1.6) mm	(1.4 x 1.5) mm
13.5nm	(3.5 x 2.7) mm	(3.6 x 2.1) mm	(1.6 x 1.6) mm
18nm	(3.4 x 2.7) mm	(2.4 x 2.8) mm	(1.3 x 1.6) mm

Fig. 8. Beam profiles at the pinhole plate. The left column shows the back-propagation with MrBeam while the focus was set to be at the PMMA position, 1067 mm upstream. The other two columns show image recorded of the fluorescent screen attached to the pinhole plate. The center column shows the beam with KAOS at the same configuration like in the left column, except for the 8 nm acquisition. The right column shows the images of KAOS configured such, that the beam size is approximately half as large. The corresponding beam widths in D4σ (width × height) are displayed below each picture. The back-propagation images look in upstream direction, while the images of the fluorescent screen are facing downstream.
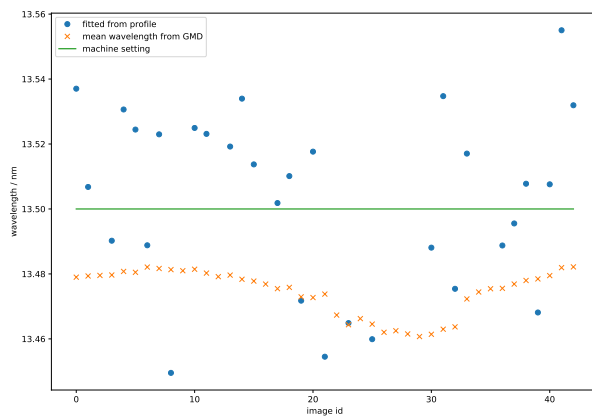
Fig. 9. Single-shot wavelength depending on the beam position. $\lambda = 13.5\,\text{nm}$, pinhole separation $d = 445\,\mu\text{m}$, orientation horizontal. rms width of the beam $\sigma_{\text{Beam}} = (405 \pm 20)\,\mu\text{m}$
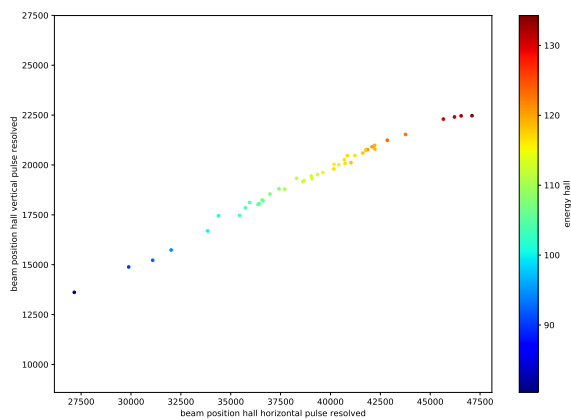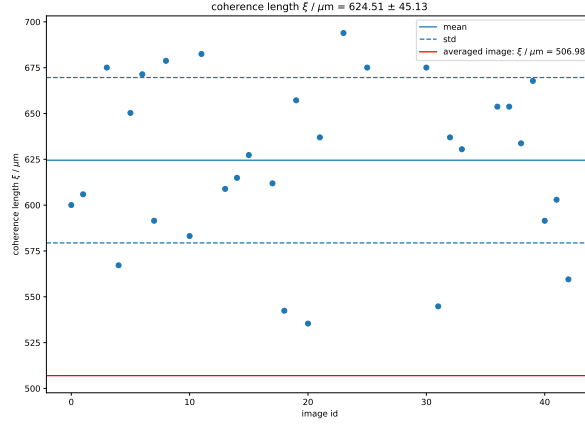

Fig. 10. Single-shot coherence energy depending on the beam position. $\lambda = 13.5\,\text{nm}$, pinhole separation $d = 445\,\mu\text{m}$, orientation horizontal. rms width of the beam $\sigma_{\text{Beam}} = (405 \pm 20)\,\mu\text{m}$

Fig. 11. Single-shot coherence length ξ calculation by applying the deconvolution-method. $\lambda = 13.5\,\text{nm}$, pinhole separation $d = 445\,\mu\text{m}$, orientation horizontal. rms width of the beam $\sigma_{\text{Beam}} = (405 \pm 20)\,\mu\text{m}$
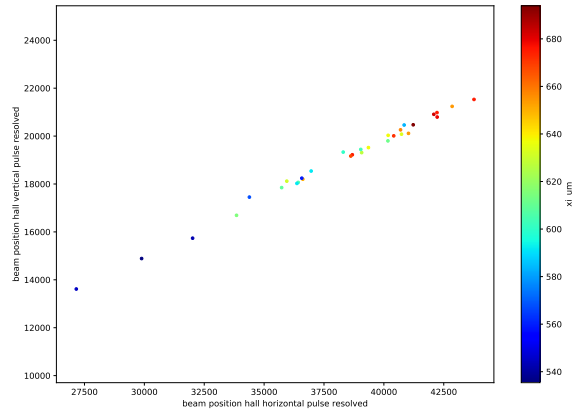
Fig. 12. Single-shot coherence length ξ depending on the beam position. $\lambda = 13.5\,\text{nm}$, pinhole separation $d = 445\,\mu\text{m}$, orientation horizontal. rms width of the beam $\sigma_{\text{Beam}} = (405 \pm 20)\,\mu\text{m}$
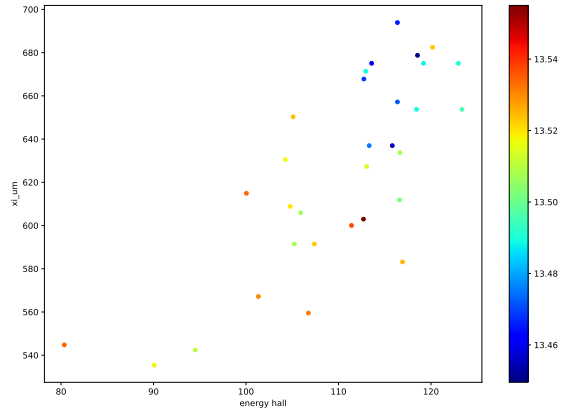
Fig. 13. Coherence length depending on the beam energy. $\lambda = 13.5\,\text{nm}$, pinhole separation $d = 445\,\mu\text{m}$, orientation horizontal. rms width of the beam $\sigma_{\text{Beam}} = (405 \pm 20)\,\mu\text{m}$
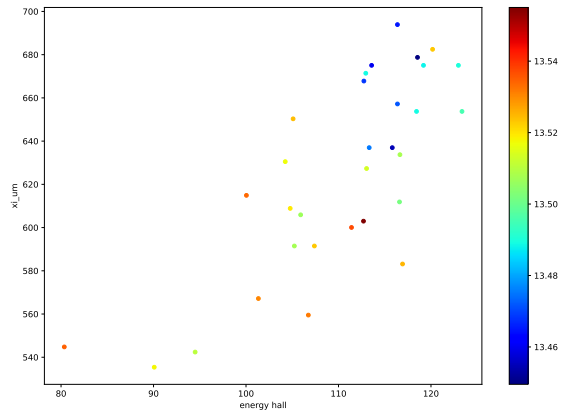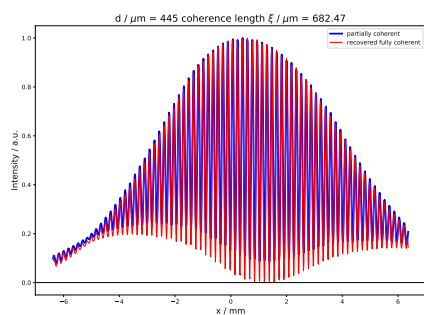

Fig. 14. Coherence length depending on the wavelength!!!. $\lambda = 13.5\,\text{nm}$, pinhole separation $d = 445\,\mu\text{m}$, orientation horizontal. rms width of the beam $\sigma_{\text{Beam}} = (405 \pm 20)\,\mu\text{m}$

[]

[]
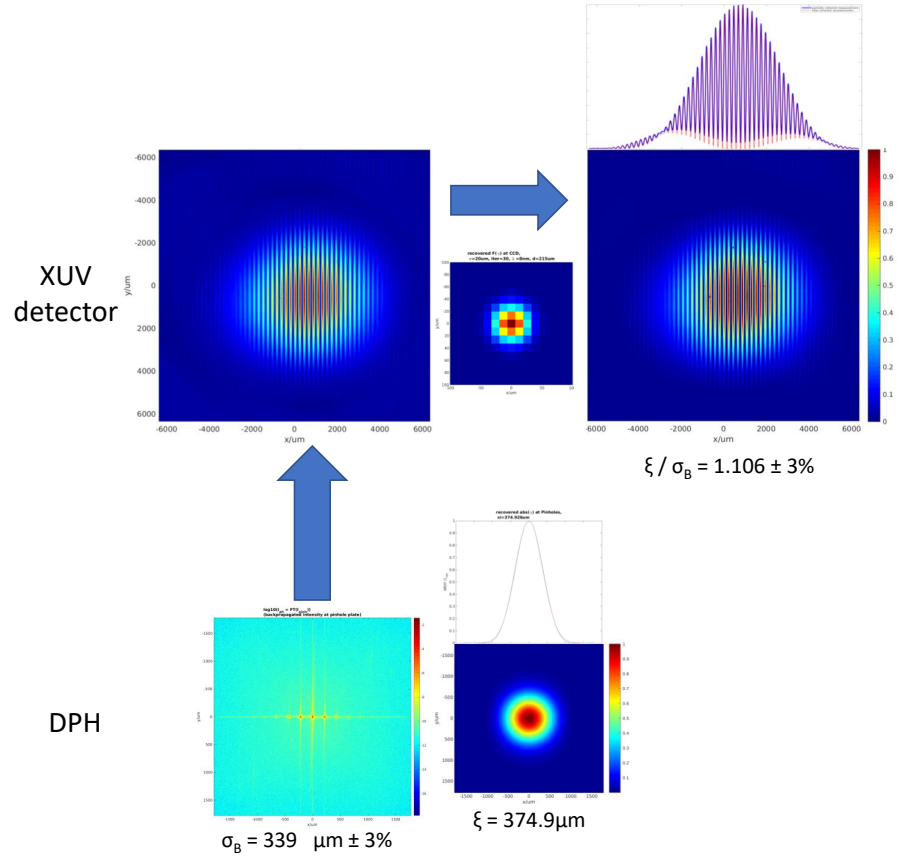

[]

XUV
detector

DPH

ξ / σ_B = 1.106 ± 3%

σ_B = 339   µm ± 3%

ξ = 374.9µm
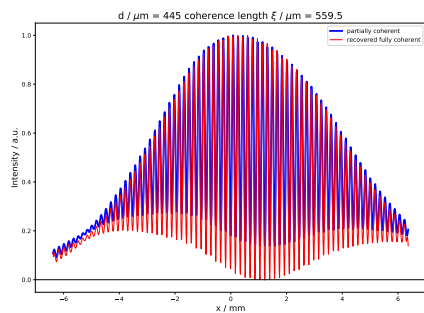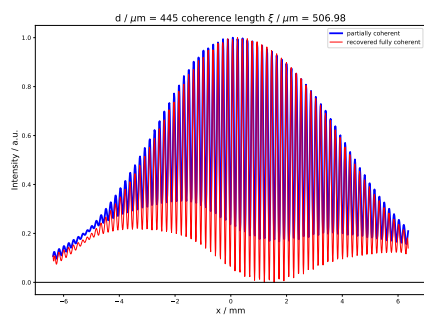
Fig. 15. Determination of the coherence length ξ by applying the deconvolution-method.
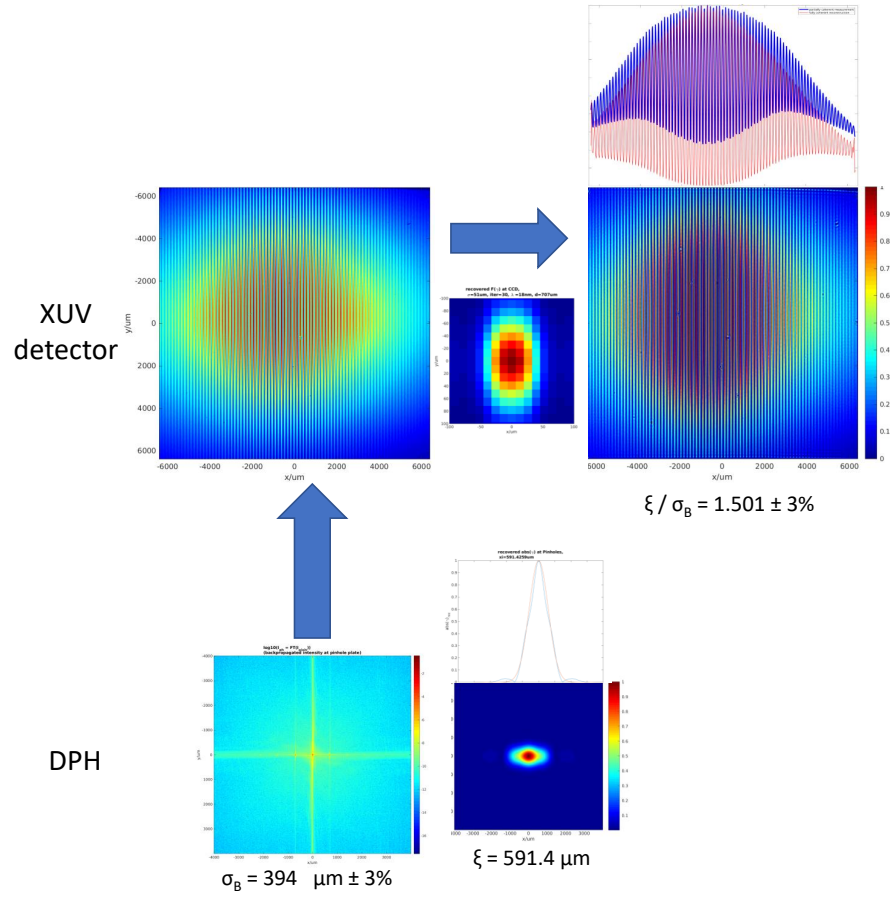λ = 8 nm, pinhole separation d = 215 µm, orientation horizontal.

XUV
detector

DPH

σ_B = 394 µm ± 3%

ξ = 591.4 µm

ξ / σ_B = 1.501 ± 3%

Fig. 16. Determination of the coherence length ξ by applying the deconvolution-method.
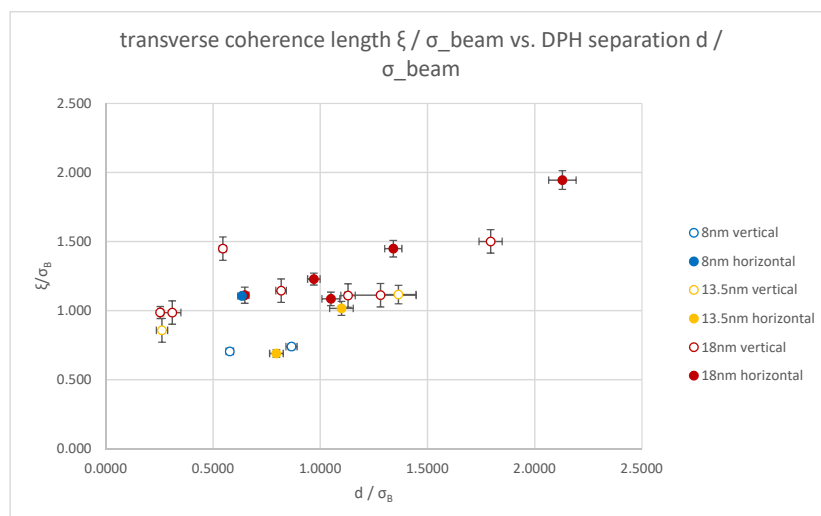λ = 18 nm, pinhole separation d = 707 µm, orientation vertical.

Fig. 17. Coherence length in relation to the pinhole separation determined from averaged-shots analysis using blinr-deconvolution method.
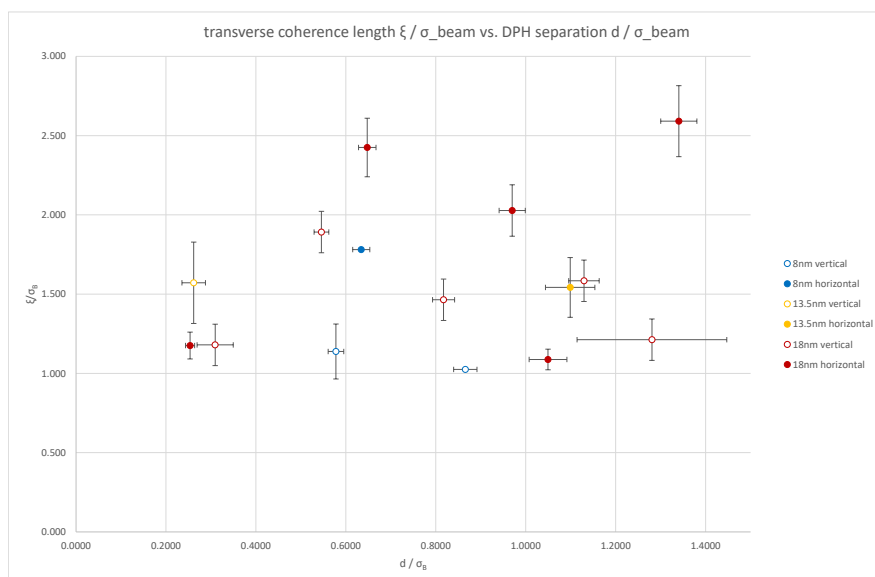

Fig. 18. Coherence length in relation to the pinhole separation determined from single-shot analysis using Wiener-deconvolution method.